Fascin-1 Is Highly Expressed Specifically in Microglia After Spinal Cord Injury and Regulates Microglial Migration

Shuisheng Yu
Second Affiliated Hospital of Anhui Medical University
Li Cheng
Second Affiliated Hospital of Anhui Medical University
Ziyu Li
Second Affiliated Hospital of Anhui Medical University
Fei Yao
Second Affiliated Hospital of Anhui Medical University
Yang Luo
Second Affiliated Hospital of Anhui Medical University
Yanchang Liu
Second Affiliated Hospital of Anhui Medical University
Zhenyu Zhu
Second Affiliated Hospital of Anhui Medical University
Meige Zheng
Second Affiliated Hospital of Anhui Medical University
Juehua Jing (jjhhu@sina.com)
Second Affiliated Hospital of Anhui Medical University

Research

Keywords: Fascin-1, microglia, migration, spinal cord injury

Posted Date: March 3rd, 2021

DOI: https://doi.org/10.21203/rs.3.rs-258359/v1

Abstract

Background

Recent research indicates that after spinal cord injury (SCI), microglia accumulate at the borders of lesions between astrocytic and fibrotic scars and perform inflammation-limiting and neuroprotective functions; however, the mechanism of microglial migration remains unclear. Fascin-1 is a key actin-bundling protein that regulates cell migration, invasion and adhesion, but its role during SCI has not been reported.

Methods

A mouse model of thoracic (T10) spinal cord compression injury was used. We employed Western blotting, and immunohistochemistry to assess expression levels of Fascin-1 protein and analyze cell localization of Fascin-1 after SCI. We employed Scratch assay and Transwell assay to evaluate the effect of Fascin-1 on the function of microglia *in vitro*.

Results

We found that at 7-14 days after SCI in mice, Fascin-1 is significantly upregulated, mainly distributed around the lesion, and specifically expressed in CX3CR1-positive microglia. However, Fascin-1 is not expressed in GFAP-positive astrocytes, NeuN-positive neurons, NG2-positive cells, PDGFRβ-positive cells, or blood-derived Mac2-positive macrophages infiltrating into the lesion core. The expression of Fascin-1 is correspondingly decreased after microglia are specifically depleted in the injured spinal cord by the colony-stimulating factor 1 receptor (CSF1R) inhibitor PLX5622. The upregulation of Fascin-1 expression is observed when microglia are activated by myelin debris *in vitro*, and microglial migration is prominently increased. The inhibition of Fascin-1 expression using small interfering RNA (siRNA) markedly suppresses the migration of microglia, but this effect can be reversed by treatment with myelin. The M1/M2 polarization of microglia does not affect the expression of Fascin-1.

Conclusions

Our results suggest that Fascin-1 is highly expressed specifically in microglia after SCI and can play an important role in the migration of microglia and the formation of microglial scars. Hence, the elucidation of this mechanism will provide novel therapeutic targets for the treatment of SCI.

1. Introduction

Spinal cord injury (SCI) induces a complex heterogeneous inflammatory response largely mediated by resident microglia and infiltrating monocyte-derived macrophages [1, 2]. It has been difficult to distinguish between activated microglia and infiltrating macrophages in the injured spinal cord, since they share many similar markers and phenotypes [3]. Recent advances in conditional gene targeting and chimeric analysis have allowed the identities and functions of these cell populations to become increasingly clear

[2, 4, 5]. It has been shown that after SCI, infiltrating macrophages expressing high Mac2 levels but low CX3CR1 levels accumulate in the lesion core, which are overloaded with myelin debris, and trigger a sustained inflammatory reaction [6, 7]. In contrast, resident microglia expressing high CX3CR1 levels accumulate around the lesion core and form a border, which is named the “microglial scar”, to seal the lesion and block the spread of damage [8]. However, the mechanism of microglial scar formation is far from clear.

Fascin-1, an actin-bundling protein, plays a key role in the assembly and stability of cell protrusions and other actin-based structures that aid in cell motility, migration and invasion [9]. A multitude of studies have shown that Fascin-1 supports the migratory and metastatic capacities of carcinomas [10–12]. In addition, it has recently been reported that Fascin-1 is upregulated predominantly in the microglia in the posterior horn of the spinal cord in a rat model of neuropathic pain and that Fascin-1 contributes to neuropathic pain by promoting inflammation [13]. However, the cellular localization and function of Fascin-1 after SCI have not been reported.

In the present study, we found that Fascin-1 was highly expressed specifically in microglia that accumulated at the lesion border after SCI. Fascin-1 expression decreased accordingly after the specific depletion of microglia in the injured spinal cord, and this effect was accompanied by disorganized astrocytic and fibrotic scars and scattered macrophages in the injured spinal cord. Fascin-1 knockdown markedly suppressed microglial migration, but this effect could be reversed by myelin treatment. Our results suggest that Fascin-1 may play a key role in microglial migration and microglial scar formation in SCI.

2. Materials And Methods

2.1 Animals

All the animal procedures were performed in accordance with the guidelines of the Institutional Animal Care and Use Committee of Anhui Medical University (No. LLSC20160052). C57BL/6J female mice at 6–8 weeks of age were purchased from the Experimental Animal Center of Anhui Medical University. The mice were housed in a temperature- and humidity-controlled room with a 12:12-light/dark cycle and allowed free access to food and water.

2.2 SCI model

All the surgical procedures were performed under pentobarbital anesthesia. The skin around the injury site was shaved and disinfected using iodophor. Subsequently, the T10 spinal cord was exposed via a dorsal laminectomy, and moderately severe crush SCIs were made using No. 5 Dumont forceps (Fine Science Tools, 11252-20, Heidelberg, Germany) ground down to a tip with a width of 0.5 mm by compressing the cord laterally from both sides for 5 s [14]. Then, twitching of the hind limbs and movement of the tail were observed, which indicated that the SCI model was successfully established. Finally, the wound was sutured with 3 − 0 silk threads. The mice with SCI were examined daily to monitor

their recovery, and their bladders were expressed manually three times a day until the return of reflexive bladder control. The sham group were subjected to laminectomy alone. The mice were sacrificed at 3, 7 and 14 days after SCI.

2.3 Microglia depletion.

To eliminate microglia, mice were administered PLX5622 (MedChemExpress, HY-114153) at 130 mg/kg by oral gavage once a day for 17 consecutive days. PLX5622 was diluted in 5% DMSO, 40% polyethylene glycol 300, 5% polysorbate 80, and 50% saline, according to the manufacturer's instructions. An equal volume of vehicle was used as the control. SCI was established on the third day after gavage.

2.4 Preparation of myelin debris

Myelin debris was isolated as previously described [15]. Briefly, 6- to 8-week-old mice were euthanized, and their brain tissues were harvested and homogenized in ice-cold 0.32 M sucrose. Myelin debris was isolated from the brain tissues by sucrose density gradient centrifugation. The endotoxin concentration of the myelin debris was below the limit of detection of the Limulus Amebocyte Lysate assay (Lonza, Switzerland). Myelin debris was added to cells at a final concentration of 1 mg/mL in all the experiments.

2.5 Cell culture and transfection.

The BV-2 microglial cell line was obtained from the American Type Culture Collection (CRL-3265, ATCC, Manassas, VA, USA) and cultured and maintained in Dulbecco's modified Eagle's medium (DMEM, HyClone, SH30021) supplemented with 10% fetal bovine serum (FBS, Gibco, 10270106), 100 U/ml penicillin and 100 g/ml streptomycin (Gibco, Grand Island, NY, USA). The cells were incubated in a humidified chamber at 37°C in a 95% O_2 and 5% CO_2 atmosphere. Small interfering RNA (siRNA) was transfected into these cells using jetPRIME (Polyplus Transfection, 114 − 15), according to the manufacturer's instructions. siRNA targeting mouse Fascin-1 (siRNA: 5'- GAUGCCAACCGUUCCAGUUTT − 3') and nonspecific control siRNA (NC) were purchased from GenePharma (Shanghai, China).

2.6 Microglial polarization

BV-2 cells were plated in poly-d-lysine (PDL, Sigma, P7280)-coated 6-well plates at a density of 1×10^6 cells/ml and cultured overnight. After serum deprivation for 24 h, the BV-2 cells were polarized toward the M1 phenotype by treatment with lipopolysaccharide (LPS; 100 ng/ml, Beyotime Biotechnology, ST1470, Shanghai, China) and IFNγ (20 ng/ml, Beyotime Biotechnology, P6137) or toward the M2 phenotype by treatment with IL-4 (20 ng/ml, Beyotime Biotechnology, P5916), and the cells were cultured for 24 h [16].

2.7 Tissue processing

For Western blot analysis, the mice were anesthetized and transcardially perfused with 0.1 M phosphate-buffered saline (PBS) to remove the blood. Spinal cord tissues of 5 mm centered at the injury site were harvested. For histological analysis, once the blood was removed, the mice were transcardially perfused with 4% paraformaldehyde (PFA), and a 5-mm portion of the spinal cord encompassing the injury epicenter was extracted and embedded in paraffin. Then, the tissues were sagittally sectioned at

thicknesses of 6 μm on a microtome (Leica RM2235). Every tenth section was collected and mounted onto a series of slides.

2.8 Immunofluorescence analysis

Immunohistochemistry. Six-micrometer, paraffin-embedded spinal cord sections were dried, dewaxed, hydrated and subjected to antigen repair. Next, 10% donkey serum albumin (DSA, Solarbio, SL050) containing 0.3% Triton X-100 (Solarbio, T8200) was added and incubated at room temperature for 1 h. Then, primary antibodies were added and incubated at 4°C overnight. The primary antibodies used were as follows: mouse anti-Fascin-1 (1:50, Santa Cruz, sc-21743), rabbit anti-Fascin-1 (1:100, Abcam, ab126772), goat anti-Iba1 (1:200, Novus Biologicals, NB100-1028), rabbit anti-CX3CR1 (1:500, Abcam, ab8021), rabbit anti-GFAP (1:100, Proteintech, 16825-1-AP), mouse anti-GFAP (1:100, Proteintech, 60190-1-Ig), goat anti-PDGFRβ (1:40, R&D Systems, AF1042-SP), rabbit anti-PDGFRβ (1:200, Abcam, ab32570), mouse anti-Mac2 (1:100, GB12246, Servicebio), rabbit anti-NG2 (1:100, Proteintech, 55027-1-AP), rabbit anti-iNOS (1:100, Affinity, AF0199), rabbit anti-Arg1 (1:100, Affinity, DF6657), and rabbit anti-NeuN (1:500, Abcam, ab177487). The secondary antibodies were diluted in 1% donkey serum in PBS and incubated for 1 h at room temperature. The following secondary antibodies were used: Alexa Fluor 488 and Alexa Fluor 594 (1:500, Thermo Fisher Scientific, A-21206, A-21202, A-21203, A-21207, A-11058). The nuclei were stained using 4',6-diamidino-2-phenylindole (DAPI) (1 μg/ml, Thermo Fisher Scientific). The fluorescence signals were obtained using an Axio Scope A1 microscope (Zeiss, Germany). ImageJ software (National Institutes of Health, Bethesda, MD, USA) was used for quantitative analysis.

Immunocytochemistry. Cells were fixed with 4% PFA for 10–15 min and blocked with 5% donkey serum in PBS for 30 min at 20–25°C. The primary antibodies (as listed above) were diluted in 1% donkey serum in PBS and incubated overnight at 4°C. The secondary antibodies (as listed above) were diluted in 1% donkey serum in PBS and incubated for 1 h at room temperature. Images were acquired as described above.

2.9 Imaging analysis and quantification

Every tenth 6-μm-thick, paraffin-embedded section was quantified, resulting in 5 analyzed slides per animal that included the entire injured spinal cord. The total number of Fascin-1$^+$, CX3CR1$^+$, and Fascin-1$^+$CX3CR1$^+$ double-positive cells in each of the sagittal sections of the spinal cord was counted under a 20× objective lens with Zeiss ZEN imaging software (Zeiss, Germany).

2.10 Western blot analysis

Tissues were homogenized in radioimmunoprecipitation assay (RIPA) buffer (Sigma, R0278) supplemented with protease inhibitors (Roche, 04693124001) and phosphatase inhibitors (Roche, 04906845001). The cells were washed with cold PBS, homogenized in RIPA buffer on ice for 30 min, and then centrifuged at 12,000 rpm at 4°C for 30 min. The protein extracts were quantified by using a Pierce BCA protein assay kit (Beyotime Biotechnology, P0010S). Aliquots of the protein samples containing equal protein concentrations were separated on 10% sodium dodecyl sulfate (SDS)-polyacrylamide gels

and subsequently transferred to polyvinylidene (PVDF) membranes. The membranes were blocked with 5% nonfat milk in Tris-buffered saline with 0.5% Tween-20 (TBST) for 1 h at room temperature and then incubated with primary antibodies, including mouse anti-GAPDH (1:2000, Proteintech, 60004-1-Ig), rabbit anti-Fascin-1 (1:5000, Abcam, ab126772), rabbit anti-iNOS (1:3000, AF0199, Affinity) and rabbit anti-CD206 (1:1000, ab64693, Abcam), at 4°C overnight. After three washes with TBST, the membranes were incubated with horseradish peroxidase (HRP)-conjugated goat anti-mouse secondary antibodies (1:10000, Sigma, A4416) and HRP-conjugated goat anti-rabbit secondary antibodies (1:10000, Sigma, A0545) for 1 h at room temperature. The protein band signals were obtained using an ECL detection kit (ECL, Thermol Biotech Inc., USA) and Tanon 5200 system (Tanon, Shanghai, China). ImageJ was used for quantification analysis. The intensity of the GAPDH bands was used for normalization.

2.11 Scratch assay

Cell migration was assessed by performing a scratch assay. Briefly, BV-2 cells were seeded into PDL-coated 6-well plates at a density of 2×10^5 cells/well and incubated for 24 h. The cell layers were scratched using a 200-μl pipette tip to form a wound-like gap. The cells were then maintained in DMEM with 2% FBS, and images were captured at 0 h, 24 h and 48 h after cell scratching. ImageJ was used to analyze the wound width.

2.12 Transwell assay

A 24-well plate containing a 3-μm chamber (Costar, 3415) was used to assess the migration abilities of the cells. BV-2 cells were transfected and activated in a PDL-coated 6-well plate before inoculation into the chamber. Then, the cells were suspended in serum-free media and seeded into the upper chamber (5×10^4 cells per chamber). The lower chamber contained complete media. After incubating for 12 h, the nonmigrating cells on the inside of the membrane were carefully removed with a cotton swab, and the migrating cells on the outside of the membrane were fixed with 4% PFA at room temperature for 20 min and stained with 0.1% crystal violet for 15 min. The cells were observed under a microscope and counted. At least 5 random fields were photographed, and the cells in each field were counted.

2.13 Statistical analysis

All the experiments were independently performed with at least three replicates and quantified in a blinded manner. The data are presented as the mean ± standard error of the mean (SEM). The statistical analysis was carried out with SPSS version 19.0 (SPSS Inc., Chicago, IL, USA) software. *Student's t* test to compare the difference between 2 groups and One-way analysis of variance followed by *Tukey's post hoc* test was used to compare differences among multiple groups. Differences were considered statistically significant if $P < 0.05$.

3. Results

3.1 Fascin-1 is significantly upregulated and distributed at the edge of the lesion core after SCI

To determine the changes in Fascin-1 expression during SCI, Western blot was used to detect the relative expression levels of Fascin-1 before and 3–14 days after SCI. As shown in Figs. 1a and 1b, Fascin-1 expression was significantly increased at 7 and 14 days after SCI compared with that before injury ($^{*}P < 0.05$ and $^{***}P < 0.001$, respectively). To further analyze the distribution of Fascin-1, we carried out immunofluorescence detection of Fascin-1 and GFAP, which is used to label the astrocytic scar formed around the injury site. The fluorescence signal of Fascin-1 was also obviously increased at 7 and 14 days after SCI and gradually accumulated at the edge of the lesion core, intermingling but not colocalizing with $GFAP^+$ astrocytic scars (Fig. 1c). These results indicate that the expression of Fascin-1 is prominently upregulated and mainly distributed at the lesion border; Fascin-1 expression has a spatiotemporal distribution pattern similar to that of microglia after SCI [8].

3.2 Fascin-1 is specifically expressed in microglia after SCI

The cellular localization of Fascin-1 was then detected by immunofluorescence staining. We found that Fascin-1 was highly colocalized with CX3CR1-labeled microglia. The percentage of $Fascin\text{-}1^+CX3CR1^+$ costained cells relative to the total number of $Fascin\text{-}1^+$ or $CX3CR1^+$ cells in the injured spinal cord reached 94.06 ± 0.82% or 87.65 ± 1.08%, respectively (Figs. 2a and 2d). These costained cells were mainly located around the SCI site (Fig. 2a), which was consistent with previous studies [8]. Fascin-1 was not expressed in the $GFAP^+$ astrocytes surrounding the lesion core or in the $PDGFR\beta^+$ pericytes accumulated in the epicenter (Figs. 2b and 2c).

Iba1 is a common marker of microglia, but during SCI, both resident microglia and infiltrating macrophages can be identified by Iba1 [6]. Our results showed that costaining of Fascin-1 and Iba1 was mainly confined to the edge of the injury site, which was consistent with the localization of microglia (Fig. 3a). Moreover, Fascin-1 was not colocalized with $Mac2^+$ macrophages located at the lesion core (Fig. 3b). In addition, Fascin-1 was not expressed in $NeuN^+$ neurons or $NG2^+$ cells in the injured area (Figs. 3c and 3d). Taken together, these results show that Fascin-1 is highly expressed specifically in microglia after SCI.

3.3 Depletion of microglia correspondingly reduces Fascin-1 expression after SCI

To confirm that Fascin-1 is derived from microglia, PLX5622, a selective inhibitor of colony-stimulating factor 1 receptor (CSF1R) that crosses the blood–brain barrier (BBB) and eradicates nearly all the microglia in the central nervous system (CNS), was administered to mice [17]. A solution containing PLX5622 was administered to mice by gavage starting 3 days prior to SCI and continuing until sacrifice. As shown in Figs. 4a and 4c, the number of $Fascin\text{-}1^+CX3CR1^+$ microglia in the PLX5622 group was

significantly decreased compared to that in the control group ($^{****}P < 0.0001$). The expression of Fascin-1 decreased accordingly with the depletion of CX3CR1^{+} microglia. The percentages of Fascin-1^{+} cells and CX3CR1^{+} cells in the PLX5622 groups relative to those in the untreated control groups were 26.14 ± 0.61% and 27.38 ± 1.07%, respectively (Fig. 4d). After the depletion of microglia, we observed that both GFAP^{+} astrocytic scars and PDGFRβ^{+} fibrotic scars became less compact and disorganized, and infiltrating Mac2^{+} macrophages were diffusely scattered outside of the lesion core (Fig. 4b). These results indicate that Fascin-1 is mainly derived from microglia after SCI. The significant upregulation of Fascin-1 may play an important role in the formation of microglial scars.

3.4 High expression of Fascin-1 can promote microglial migration

To assess the effect of Fascin-1 on the function of microglia, we cultured the BV-2 microglial cell line *in vitro*. Western blot (Figs. 5a and 5b) and immunocytochemistry (Fig. 5c) analyses revealed that compared to the negative controls, Fascin-1 siRNA (siFascin-1) could knockdown the expression of Fascin-1, while myelin treatment could upregulate the expression of Fascin-1. The migration ability of the microglia was reduced after Fascin-1 knockdown but enhanced by myelin addition, as observed by scratch and Transwell assays (Fig. 6). Furthermore, the inhibition of Fascin-1 expression and microglial migration using siFascin-1 could be reversed by treatment with myelin (Figs. 5 and 6). These results suggest that Fascin-1 can regulate microglial migration.

3.5 Polarization of microglia does not affect the expression of Fascin-1

Previous studies have shown that microglia can be polarized into either a pro- inflammatory (M1) or anti-inflammatory (M2) phenotype and involved in the regulation of the SCI microenvironment [18]. Next, we detected the effect of microglial polarization on Fascin-1 expression. Western blot analysis showed that M1 microglia significantly expressed iNOS and M2 microglia significantly expressed CD206 (Figs. 7a and 7b). In addition, immunocytochemistry was used to further confirm the reliability of microglial polarization (Figs. 7c and 7d). However, the expression of Fascin-1 in the polarized microglial populations was not significantly different (Fig. 7). The results show that microglial polarization has no effect on the expression of Fascin-1.

4. Discussion

Microglia, the resident immune cells of the CNS, are cells that rapidly respond to CNS injury [19, 20]. Following SCI, these cells migrate or project processes toward sites of injury, where they release neurotrophic agents and confer neuroprotection [8, 21]. In this study, we demonstrate that the actin-bundling protein Fascin-1 is highly expressed specifically in microglia after SCI and is indispensable for microglial migration. The expression of Fascin-1 is correspondingly reduced after the specific elimination

of microglia by the CSF1R inhibitor PLX5622, and this effect is associated with disordered astrocytic and fibrotic scars and widespread macrophages in the injured spinal cord. Thus, we highlight that Fascin-1 can play a vital role in regulating microglial migration and microglial scar formation after SCI.

The proliferation of $CX3CR1^{+}$ residual microglia has been observed beginning at 3 days after SCI [6]. Microglia are rapidly recruited around the lesion epicenter, exhibit a round morphology, and upregulate the lysosome-associated protein CD68, which suggests a potential increase in their phagocytic activity. Moreover, microglia continue to proliferate and accumulate around the site of the lesion epicenter, peaking at 14 days after SCI and forming microglial scars [8]. Our results also show that Fascin-1 is prominently expressed in microglia beginning at 3 days and peaks at 14 days after SCI. Olah et al. determined the global gene expression changes in microglia during demyelination and remyelination via microarray analysis, and the results suggested that the primary functions of CNS-resident microglia are repair and maintenance of tissue homeostasis [22]. Using the lysozyme M EGFP-knock-in mouse, in which the expression of EGFP is specifically promoted in hematogenous macrophages but in not microglia, Greenhalgh and David showed that microglia are the predominant cells that contact and phagocytose damaged and degenerating tissue 3 days after SCI; however, $EGFP^{+}$ infiltrating macrophages are less efficient at processing CNS debris, and their death *in situ* may contribute to secondary damage after SCI [23]. In the latest study, the transplantation of $CX3CR1^{GFP/+}$ neonatal microglia or adult microglia treated with peptidase inhibitors into the spinal cord lesions of adult mice improved wound healing and axon regeneration [24]. Consistent with previous studies, our results also confirmed that $CX3CR1^{+}$ microglia surround $Mac2^{+}$ macrophages at 14 days after SCI. Moreover, when microglia are eliminated, the compact form of astrocytic scars is destroyed, and macrophages are scattered, indicating that microglial scarring plays an important role in maintaining astrocytic scarring and limiting inflammation. However, the mechanism by which microglia accumulate to form protective scars remains unclear.

Fascin-1 is a cytoskeleton-organizing protein localized at the core actin bundles within microvillar projections and filopodial extensions of migrating cells [25, 26]. Fascin-1 is expressed in neurons, dendritic cells and myofibroblasts [9, 27]. Fascin-1 can promote structural changes in cell membranes and affect the integrity of intercellular interactions to promote the invasion and metastasis of tumor cells [28, 29]. Compared with the vector control, overexpression of Fascin-1 in colonic epithelial cells increases their motility on two-dimensional laminin surfaces and enhances their migration through extracellular matrix (ECM)-coated filters [30]. However, tumor metastasis of lung adenocarcinoma cells is blocked when Fascin-1 is knocked out with short hairpin RNA (shRNA), indicating that Fascin-1 plays a mechanical role in driving tumor cell migration and invasion [31]. These studies show that Fascin-1 may be essential for cell migration. In the CNS, Fascin-1 plays an indispensable role in the development and polarization of filopodia (early neuritis) and growth cones, which can guide neurite outgrowth and branching [32]. Fascin-1 can also bind to MHC-II and B7-2 to play a role in the antigen presentation of dendritic cells [27]. B Wang et al. studied the role of microglia in neuropathic pain and found that microglia upregulate the expression of Fascin-1 in the posterior horn of the L4-L6 spinal cord, which then

participates in the process of antigen presentation and the regulation of the secretion of the inflammatory factors TNF-α and IL-6 [13]. Considering that microglia are professional antigen-presenting cells in the CNS, we hypothesized that Fascin-1 may also regulate the migration and functional activity of microglia after SCI. Our data show that Fascin-1 is highly expressed specifically in microglia after SCI but not in neurons, astrocytes, $NG2^+$ cells, pericytes, or blood-derived macrophages. Hence, Fascin-1 is expected to become a specific marker of microglia during CNS injury. Fascin-1 also plays an important role in regulating the migration of microglia, as demonstrated by gain- and loss-of-function studies. Thus, Fascin-1 may be a key regulatory protein for the formation of microglial scars, which can envelop inflammatory macrophages and promote the repair of SCI.

CX3CR1 is a receptor of fractalkine and directly mediates the adhesion and migration of leukocytes and microglia [33, 34]. Wang X et al. labeled infiltrating macrophages in chimeric mice and showed that after SCI, infiltrating macrophages expressing higher Mac2 levels accumulated at the epicenter and microglia expressing higher CX3CR1 levels were distributed at the edges of the lesion [6]. In $CX3CR1^{-/-}$ mice with demyelinating disease, the clearance of myelin debris by microglia was substantially inhibited, affecting the integrity of the axon and myelin sheaths and thus preventing remyelination [35]. Moreover, we found that Fascin-1 is expressed specifically in $CX3CR1^+$ microglia after SCI, and the expression of Fascin-1 decreases accordingly with the depletion of $CX3CR1^+$ microglia. We hypothesize that CX3CR1 may be the upstream regulator of Fascin-1 and mediate the changes in its expression during SCI.

Microglia play an important role in inflammation and nerve remodeling [36]. It has been shown that microglia can be polarized into M1-neurotoxic or M2-neuroprotective states and produce a variety of cytokines involved in the regulation of the SCI microenvironment [37, 38]. However, in this study, we found that the polarization of microglia does not affect the expression of Fascin-1.

5. Conclusion

In summary, this study found that Fascin-1 is highly expressed specifically in microglia after SCI and can regulate microglial migration. The migration and accumulation of microglia at the lesion border after SCI may be closely related to the specific upregulation and cellular localization of Fascin-1. Hence, the elucidation of this mechanism will provide new insights into novel therapeutic targets for the treatment of SCI.

Abbreviations

SCI: Spinal cord injury; CSF1R: Colony-stimulating factor 1 receptor; siRNA: Small interfering RNA; DMEM: Dulbecco's modified Eagle's medium; FBS: Fetal bovine serum; NC: Nonspecific control; PDL: Poly-d-lysine; LPS: Lipopolysaccharide; PBS: Phosphate-buffered saline; PFA: Paraformaldehyde; DSA: Donkey serum albumin; DAPI: 4',6-diamidino-2-phenylindole; ANOVA: Analysis of variance; RIPA: Radioimmunoprecipitation; TBST: Tris-buffered saline with 0.5% Tween-20; HRP: Horseradish peroxidase; CNS: Central nervous system ; BBB: Blood–brain barrier; ECM: Extracellular matrix.

Declarations

Ethics approval and consent to participate

Ethics approval was obtained by the Ethics Committee of Anhui Medical University (No. LLSC20160052).

Consent for publication

Not applicable.

Availability of data and materials

The data that support the findings of this study are available from the corresponding author upon reasonable request.

Competing interests

The authors declare that there is no conflict of interest regarding the publication of this article.

Authors' contributions

SY and JJ conceived and designed the project. SY, ZL, FY, and YL performed research. SY, LC, YCL, and ZZ analyzed data, and prepared figures. SY and MZ wrote the manuscript. All authors read and approved the final manuscript.

Funding

This work was supported by the National Natural Science Foundation of China (No. 81801220 and 81671204) and Key Research and Development Projects of Anhui Province (No. 202004j07020042).

Acknowledgments

We would like to thank the Research Center of the Second Affiliated Hospital of Anhui Medical University for providing technical assistance.

Authors' information

Department of Orthopaedics, The Second Hospital of Anhui Medical University, No. 678 Furong Road, Hefei 230601, Anhui, China

References

1. Davies CL, Miron VE: Distinct origins, gene expression and function of microglia and monocyte-derived macrophages in CNS myelin injury and regeneration.*Clinical immunology* 2018, 189:57-62.

2. Milich LM, Ryan CB, Lee JK: The origin, fate, and contribution of macrophages to spinal cord injury pathology.*Acta Neuropathol* 2019, 137:785-797.
3. David S, Kroner A: Repertoire of microglial and macrophage responses after spinal cord injury.*Nature reviews Neuroscience* 2011, 12:388-399.
4. Zhou X, Wahane S, Friedl M-S, Kluge M, Friedel CC, Avrampou K, Zachariou V, Guo L, Zhang B, He X: Microglia and macrophages promote corralling, wound compaction and recovery after spinal cord injury via Plexin-B2.*Nature Neuroscience* 2020, 23:337-350.
5. Russo MV, Latour LL, McGavern DB: Distinct myeloid cell subsets promote meningeal remodeling and vascular repair after mild traumatic brain injury.*Nature immunology* 2018, 19:442-452.
6. Wang X, Cao K, Sun X, Chen Y, Duan Z, Sun L, Guo L, Bai P, Sun D, Fan J, et al: Macrophages in spinal cord injury: phenotypic and functional change from exposure to myelin debris.*Glia* 2015, 63:635-651.
7. Zhou X, He X, Ren Y: Function of microglia and macrophages in secondary damage after spinal cord injury.*Neural regeneration research* 2014, 9:1787-1795.
8. Bellver-Landete V, Bretheau F, Mailhot B, Vallières N, Lessard M, Janelle M-E, Vernoux N, Tremblay M-È, Fuehrmann T, Shoichet MS: Microglia are an essential component of the neuroprotective scar that forms after spinal cord injury.*Nature communications* 2019, 10:1-18.
9. Tan V, Lewis S, Adams J, Martin R: Association of fascin-1 with mortality, disease progression and metastasis in carcinomas: a systematic review and meta-analysis.*BMC medicine* 2013, 11:52.
10. Gao R, Zhang N, Yang J, Zhu Y, Zhang Z, Wang J, Xu X, Li Z, Liu X, Li Z, et al: Long non-coding RNA ZEB1-AS1 regulates miR-200b/FSCN1 signaling and enhances migration and invasion induced by TGF-β1 in bladder cancer cells.*Journal of experimental & clinical cancer research : CR* 2019, 38:111.
11. Hashimoto Y, Kim D, Adams J: The roles of fascins in health and disease.*The Journal of pathology* 2011, 224:289-300.
12. Ma Y, Li A, Faller W, Libertini S, Fiorito F, Gillespie D, Sansom O, Yamashiro S, Machesky L: Fascin 1 is transiently expressed in mouse melanoblasts during development and promotes migration and proliferation.*Development (Cambridge, England)* 2013, 140:2203-2211.
13. Wang B, Fan B, Dai Q, Xu X, Jiang P, Zhu L, Dai H, Yao Z, Xu Z, Liu X: Fascin-1 Contributes to Neuropathic Pain by Promoting Inflammation in Rat Spinal Cord.*Neurochemical research* 2018, 43:287-296.
14. Wanner I, Anderson M, Song B, Levine J, Fernandez A, Gray-Thompson Z, Ao Y, Sofroniew M: Glial scar borders are formed by newly proliferated, elongated astrocytes that interact to corral inflammatory and fibrotic cells via STAT3-dependent mechanisms after spinal cord injury.*The Journal of neuroscience : the official journal of the Society for Neuroscience* 2013, 33:12870-12886.
15. Rolfe A, Bosco D, Broussard E, Ren Y: In Vitro Phagocytosis of Myelin Debris by Bone Marrow-Derived Macrophages.*Journal of visualized experiments : JoVE* 2017.
16. Kigerl K, Gensel J, Ankeny D, Alexander J, Donnelly D, Popovich P: Identification of two distinct macrophage subsets with divergent effects causing either neurotoxicity or regeneration in the injured

mouse spinal cord.*The Journal of neuroscience : the official journal of the Society for Neuroscience* 2009, 29:13435-13444.

17. Huang Y, Xu Z, Xiong S, Sun F, Qin G, Hu G, Wang J, Zhao L, Liang Y, Wu T, et al: Repopulated microglia are solely derived from the proliferation of residual microglia after acute depletion.*Nature neuroscience* 2018, 21:530-540.
18. Francos-Quijorna I, Amo-Aparicio J, Martinez-Muriana A, López-Vales RJG: IL-4 drives microglia and macrophages toward a phenotype conducive for tissue repair and functional recovery after spinal cord injury.*Glia* 2016, 64:2079-2092.
19. Nimmerjahn A, Kirchhoff F, Helmchen F: Resting microglial cells are highly dynamic surveillants of brain parenchyma in vivo.*Science (New York, NY)* 2005, 308:1314-1318.
20. Davalos D, Grutzendler J, Yang G, Kim J, Zuo Y, Jung S, Littman D, Dustin M, Gan W: ATP mediates rapid microglial response to local brain injury in vivo.*Nature neuroscience* 2005, 8:752-758.
21. Plemel JR, Stratton JA, Michaels NJ, Rawji KS, Zhang E, Sinha S, Baaklini CS, Dong Y, Ho M, Thorburn K: Microglia response following acute demyelination is heterogeneous and limits infiltrating macrophage dispersion.*Science Advances* 2020, 6:eaay6324.
22. Olah M, Amor S, Brouwer N, Vinet J, Eggen B, Biber K, Boddeke H: Identification of a microglia phenotype supportive of remyelination.*Glia* 2012, 60:306-321.
23. Greenhalgh A, David S: Differences in the phagocytic response of microglia and peripheral macrophages after spinal cord injury and its effects on cell death.*The Journal of neuroscience : the official journal of the Society for Neuroscience* 2014, 34:6316-6322.
24. Li Y, He X, Kawaguchi R, Zhang Y, Wang Q, Monavarfeshani A, Yang Z, Chen B, Shi Z, Meng H: Microglia-organized scar-free spinal cord repair in neonatal mice.*Nature* 2020:1-6.
25. Ishikawa R, Sakamoto T, Ando T, Higashi-Fujime S, Kohama K: Polarized actin bundles formed by human fascin-1: their sliding and disassembly on myosin II and myosin V in vitro.*Journal of neurochemistry* 2003, 87:676-685.
26. Hayashi Y, Toda K, Saibara T, Okamoto S, Osanai M, Enzan H, Lee G-H: Expression of fascin-1, an actin-bundling protein, in migrating hepatoblasts during rat liver development.*Cell and tissue research* 2008, 334:219-226.
27. Al-Alwan MM, Rowden G, Lee TD, West KA: Fascin is involved in the antigen presentation activity of mature dendritic cells.*The Journal of Immunology* 2001, 166:338-345.
28. Kim M-Y, Oskarsson T, Acharyya S, Nguyen DX, Zhang XH-F, Norton L, Massagué J: Tumor self-seeding by circulating cancer cells.*Cell* 2009, 139:1315-1326.
29. Hashimoto Y, Loftis DW, Adams JC: Fascin-1 promoter activity is regulated by CREB and the aryl hydrocarbon receptor in human carcinoma cells.*PLoS One* 2009, 4:e5130.
30. Hashimoto Y, Skacel M, Adams JC: Roles of fascin in human carcinoma motility and signaling: prospects for a novel biomarker?*The international journal of biochemistry & cell biology* 2005, 37:1787-1804.

31. Lin S, Huang C, Gunda V, Sun J, Chellappan S, Li Z, Izumi V, Fang B, Koomen J, Singh P, et al: Fascin Controls Metastatic Colonization and Mitochondrial Oxidative Phosphorylation by Remodeling Mitochondrial Actin Filaments.*Cell reports* 2019, 28:2824-2836.e2828.
32. Pak C, Flynn K, Bamburg J: Actin-binding proteins take the reins in growth cones.*Nature reviews Neuroscience* 2008, 9:136-147.
33. Chidambaram H, Das R, Chinnathambi SJC, bioscience: Interaction of Tau with the chemokine receptor, CX3CR1 and its effect on microglial activation, migration and proliferation.*Cell & bioscience* 2020, 10:1-9.
34. White G, Greaves DJA, thrombosis,, biology v: Fractalkine: a survivor's guide: chemokines as antiapoptotic mediators.*Arteriosclerosis, thrombosis, and vascular biology* 2012, 32:589-594.
35. Lampron A, Larochelle A, Laflamme N, Préfontaine P, Plante M, Sánchez M, Yong V, Stys P, Tremblay M, Rivest S: Inefficient clearance of myelin debris by microglia impairs remyelinating processes.*The Journal of experimental medicine* 2015, 212:481-495.
36. Hambardzumyan D, Gutmann DH, Kettenmann H: The role of microglia and macrophages in glioma maintenance and progression.*Nature neuroscience* 2016, 19:20.
37. Han D, Yu Z, Liu W, Yin D, Pu Y, Feng J, Yuan Y, Huang A, Cao L, He C: Plasma Hemopexin ameliorates murine spinal cord injury by switching microglia from the M1 state to the M2 state.*Cell death & disease* 2018, 9:1-16.
38. Hu X, Leak R, Shi Y, Suenaga J, Gao Y, Zheng P, Chen JJNrN: Microglial and macrophage polarization—new prospects for brain repair.*Nature Reviews Neurology* 2015, 11:56-64.

Figures

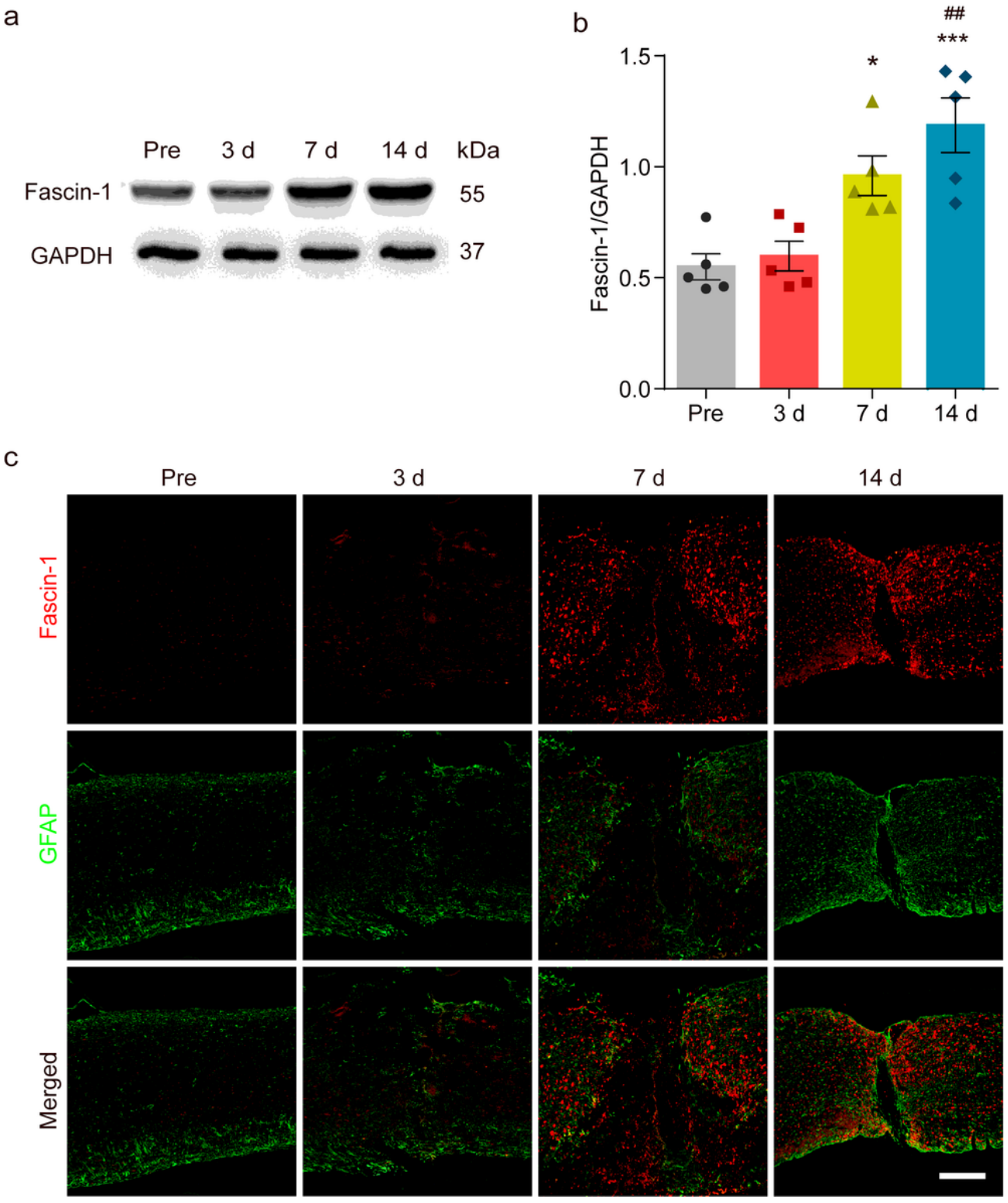

Figure 1

Fascin-1 is prominently expressed and accumulates at the lesion border after SCI. a Western blot analysis shows significant upregulation of Fascin-1 at 7 and 14 days after injury compared to the control (pre-operation, Pre). b Quantitative analysis of Fascin-1 expression in a. The blots (n = 5 per group) were quantified by a densitometric method using ImageJ software. GAPDH was used as the loading control. The results are expressed as the mean ± SEM. *** P < 0.001 (14 days vs. Pre); * P < 0.05 (7 days vs. Pre);

P < 0.01 (14 days vs. 3 days). c Double immunofluorescence labeling of spinal cord sagittal sections showing the spatiotemporal distribution of Fascin-1 (Red) and GFAP (Green) at Pre and 3, 7, and 14 days after injury. Scale bar: 50 μm.

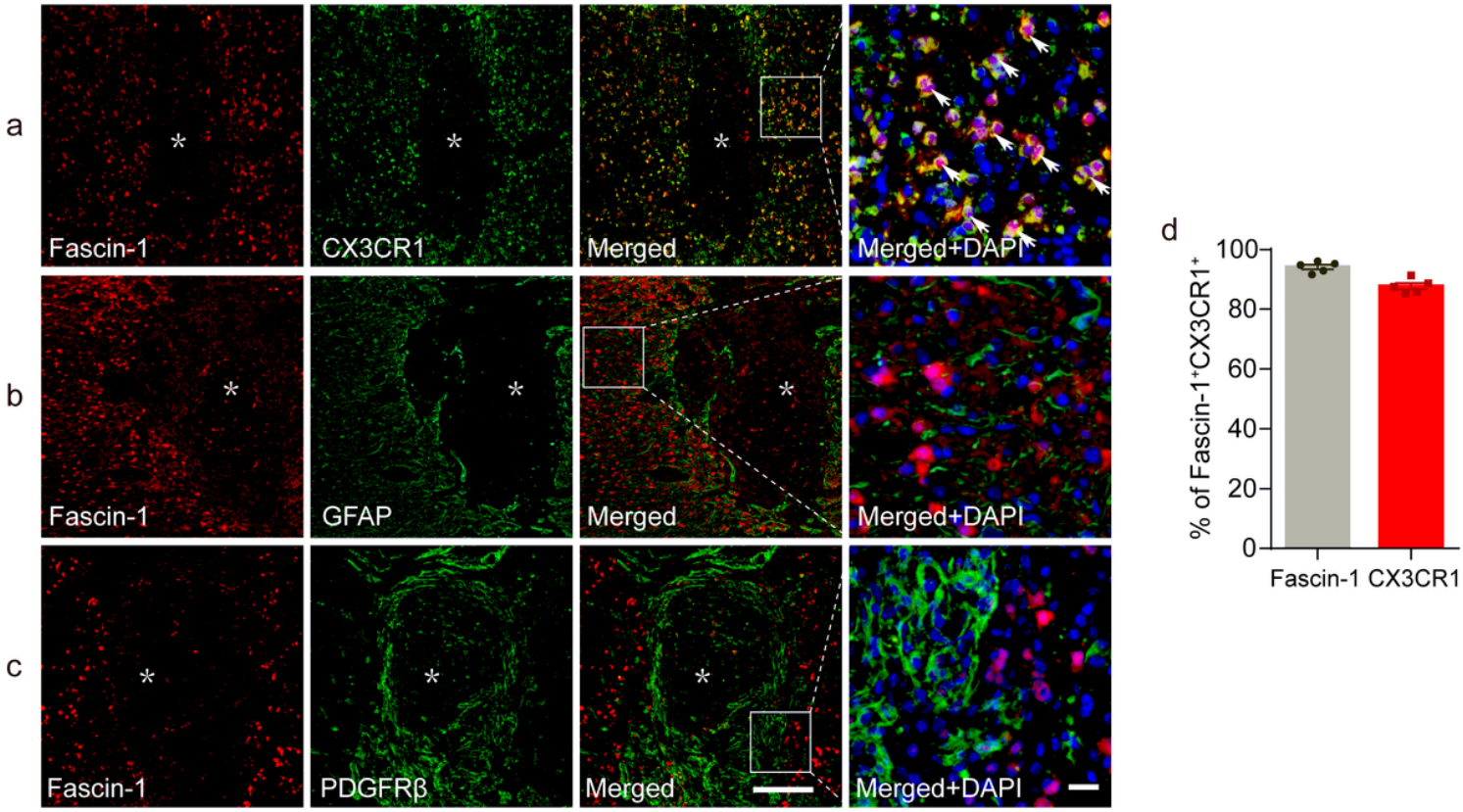

Figure 2

Fascin-1 is specifically expressed in CX3CR1+ microglia but not in GFAP+ astrocytes or PDGFRβ+ epicenter-located pericytes at 14 days after SCI. a Representative immunofluorescence images of Fascin-1 (Red) and CX3CR1 (Green). Colocalization of the proteins is shown in yellow. Nuclear staining (DAPI) is shown in blue, and white arrowheads indicate the colocalization observed with a 40× objective lens. b Representative immunofluorescence images of Fascin-1 (Red), GFAP (Green) and DAPI (Blue) showing no apparent colocalization of staining. c Representative immunofluorescence images of Fascin-1 (Red), PDGFRβ (Green) and DAPI (Blue) showing no apparent colocalization of staining. The asterisks indicate the lesion epicenter. Scale bars: low magnification, 20 μm; higher magnification, 2 μm. d Percentage of Fascin-1+CX3CR1+ cells relative to the total number of Fasicn-1+ or CX3CR1+ cells in the injured spinal cord. The data are presented as the mean ± SEM (n = 5 independent experiments).

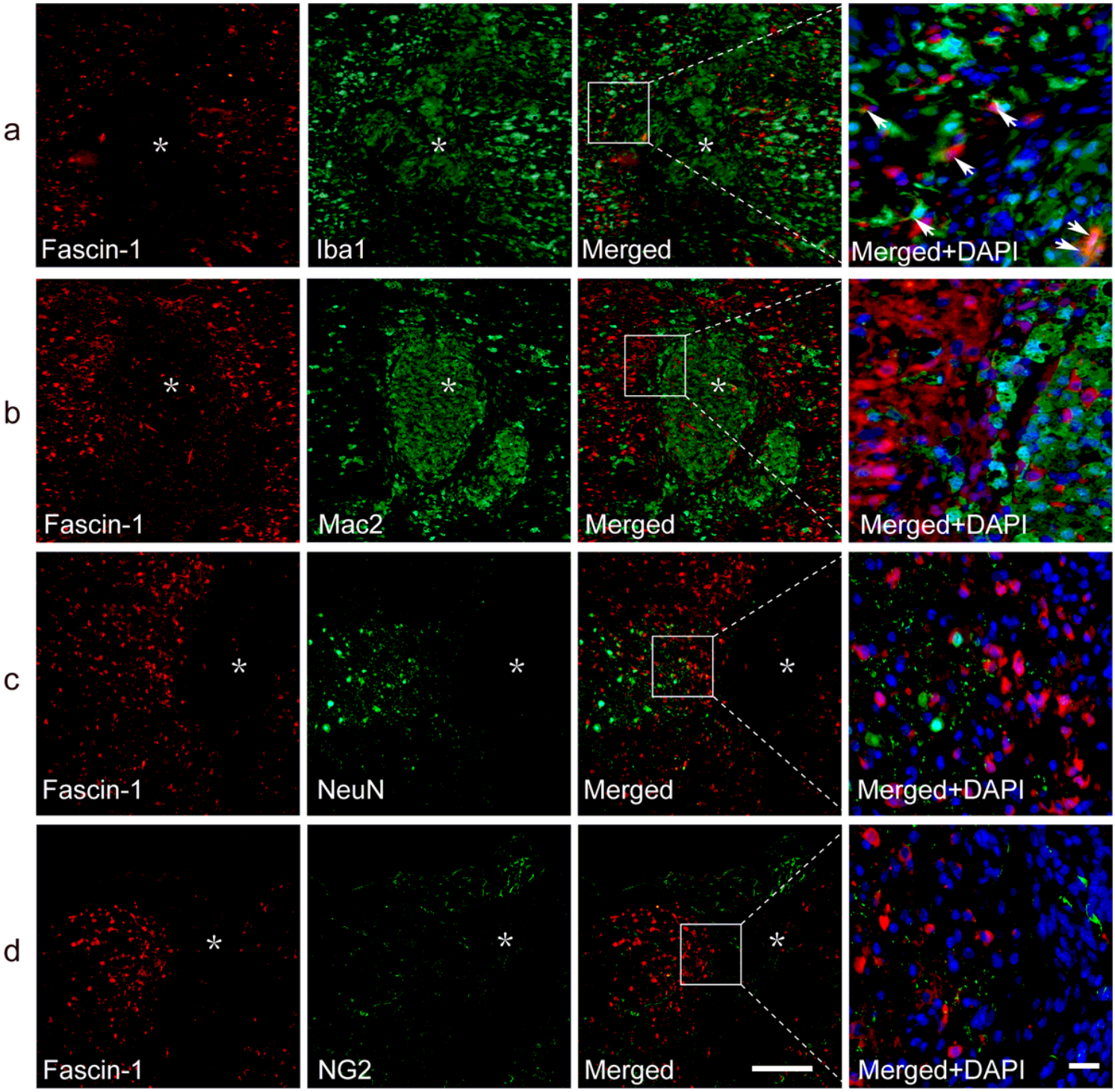

Figure 3

Fascin-1 is expressed partly in Iba1+ cells around the lesion but not in infiltrating Mac2+ macrophages, NeuN+ neurons or NG2+ cells in the injured spinal cord at 14 days. a Representative immunofluorescence images of Fascin-1 (Red) and Iba1 (Green). Arrowheads indicate the colocalization observed with a 40× objective lens. b, c, d Representative immunofluorescence images of Fascin-1 (Red) staining with Mac2, NeuN, and NG2 (Green) staining, respectively, showing no apparent colocalization of staining. The asterisks indicate the lesion epicenter. Nuclear staining with DAPI is shown (Blue). Scale bars: low magnification, 20 μm; higher magnification, 2 μm.

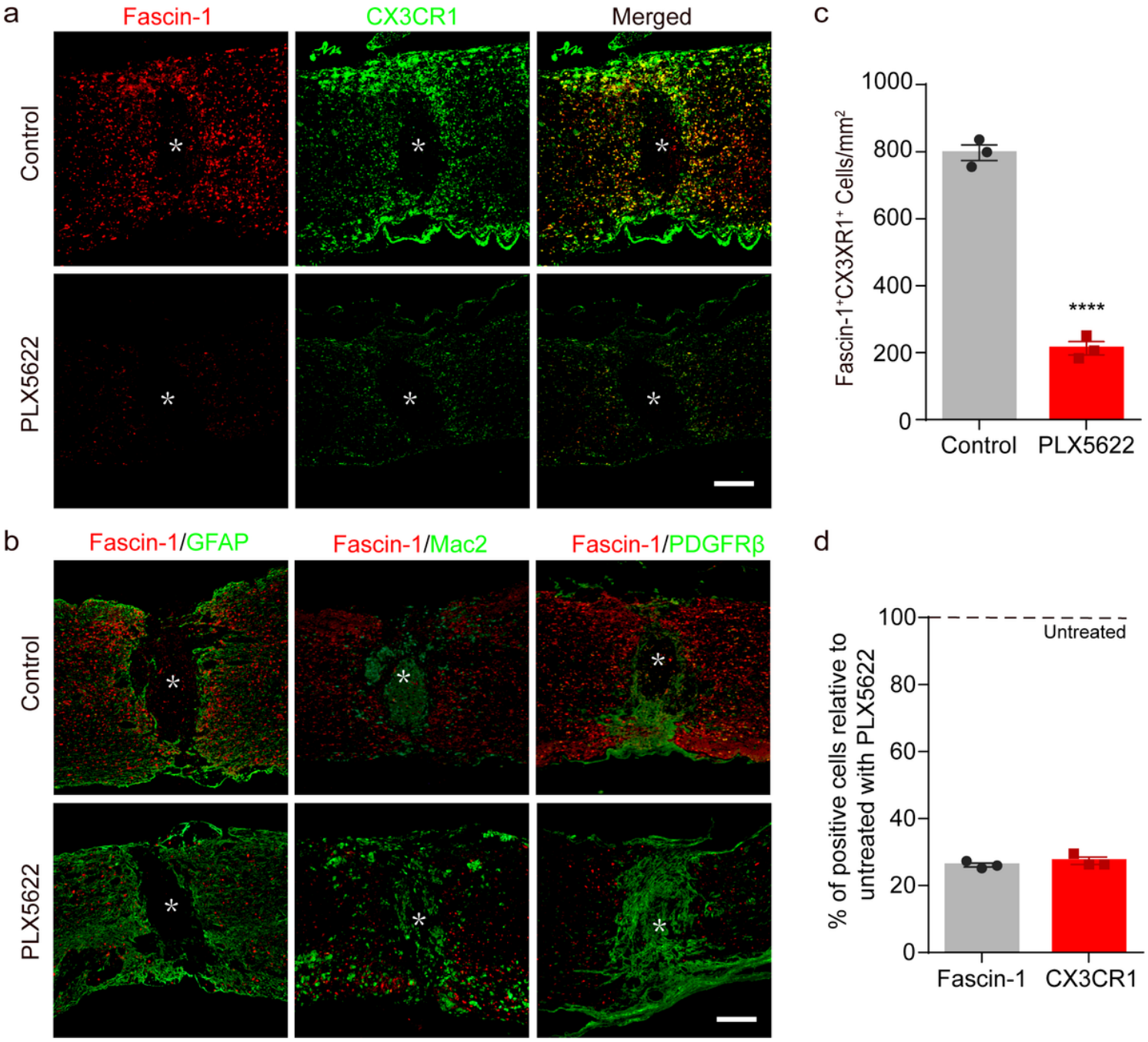

Figure 4

The elimination of microglia by PLX5622 treatment results in correspondingly reduced Fascin-1 expression, disorganized astrocytic and fibrotic scars, and scattered macrophages in the injured spinal cord at 14 days. a Representative fluorescence images of Fascin-1 (Red) and CX3CR1 (Green) immunostaining showing a consistent reduction in Fascin-1 expression with the elimination of microglia after treatment with PLX5622 compared to vehicle (control). The asterisks indicate the lesion epicenter. Scale bar: 50 μm. b Representative immunofluorescence images of Fascin-1 (Red) and GFAP (Green), Fascin-1 (Red) and Mac2 (Green), Fascin-1 (Red) and PDGFRβ (Green) at the lesion sites of mice treated with vehicle (control) or PLX5622. After the elimination of microglia using PLX5622, the compact GFAP+ astrocytic scars and PDGFRβ+ fibrotic scars are disrupted, with clusters of Mac2+ macrophages

spreading outside of the lesion core. The asterisks indicate the lesion epicenter. Scale bar: 50 μm. c Quantification of the number of Fascin-1+ CX3CR1+ microglia in the control and PLX5622 groups (n = 3 per group). The results are expressed as the mean ± SEM. **** P < 0.0001. d Percentage of surviving Fascin-1+ or CX3CR1+ cells in the PLX5622 groups relative to that the untreated control groups (n = 3 per group).

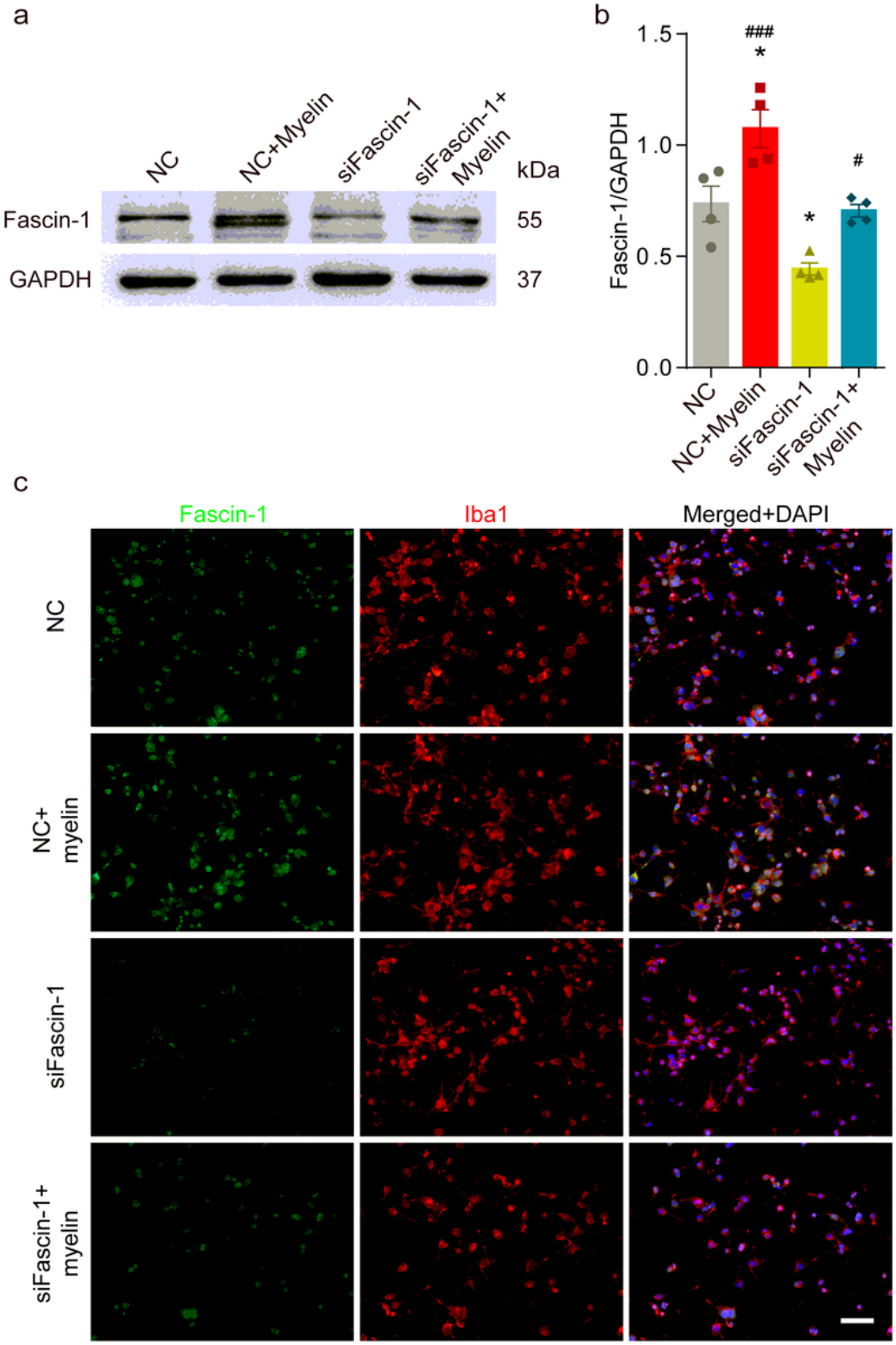

Figure 5

Inhibition of Fascin-1 expression using siRNA in BV-2 microglia can be partly rescued by treatment with myelin. a Western blot analysis shows that compared to the nonspecific control (NC), Fascin-1 siRNA (siFascin-1) could knockdown the expression of Fascin-1, while myelin treatment could upregulate the expression of Fascin-1. b Quantitative analysis of Fascin-1 expression in (a). GAPDH was used as the loading control. The blots (n = 4 per group) were quantified as previously described. The results are expressed as the mean ± SEM. * P < 0.05 (NC+Myelin or siFascin-1 vs. NC); # P < 0.05 (NC+Myelin vs. siFascin-1), ### P < 0.001 (siFascin-1+Myelin vs. siFascin-1). c BV-2 cells were transfected with nonspecific control (NC) siRNA or siFascin-1 for 24 h and then treated with or without myelin for an additional 24 h in complete medium. Representative immunofluorescence images of Fascin-1 (Green) and Iba1 (Red) are shown. DAPI (Blue) was used to stain the nuclei. Scale bar: 10 μm.

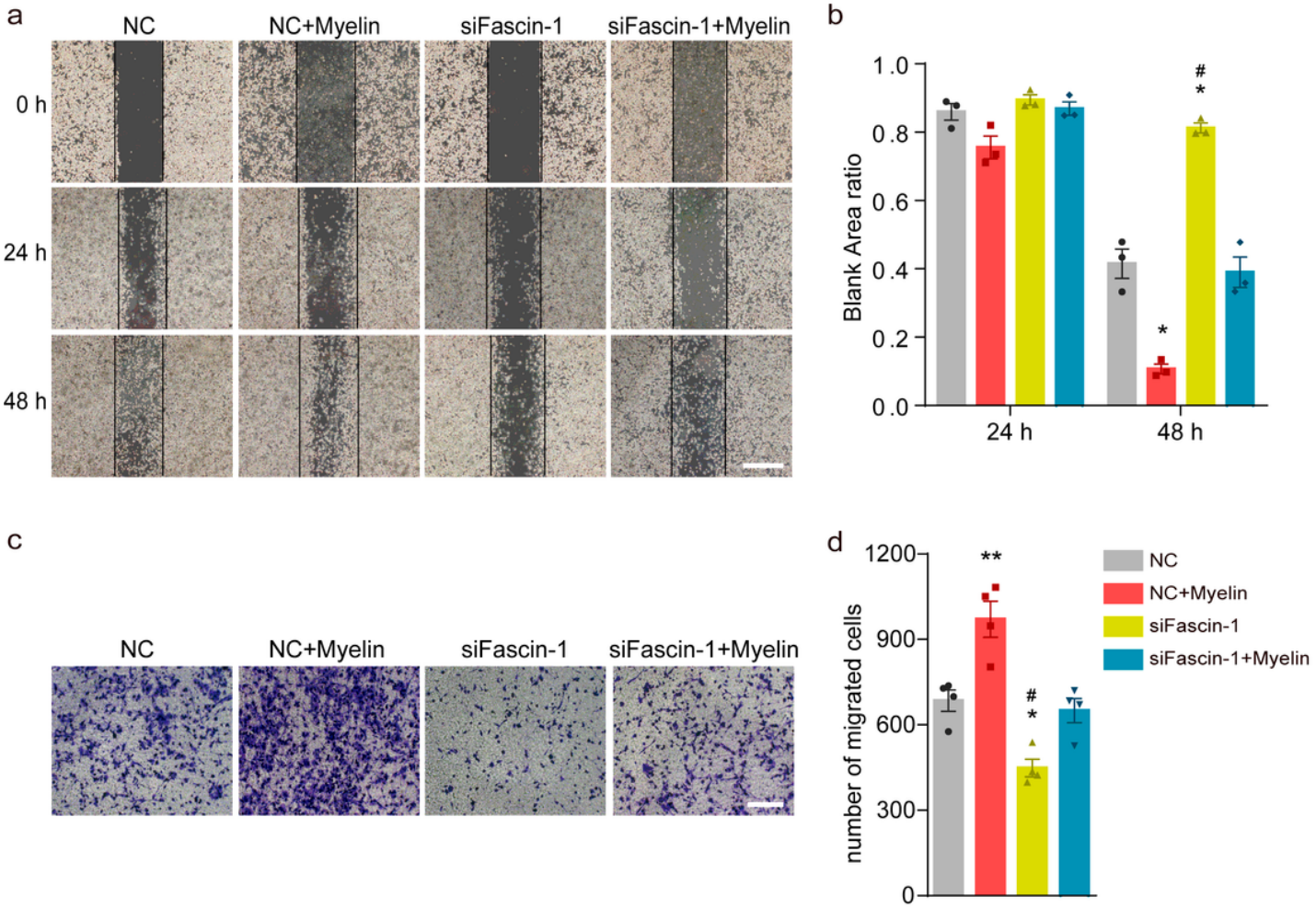

Figure 6

Fascin-1 promotes the migration of microglia in vitro. a For the scratch assay, cell migration was recorded at 0, 24 and 48 h after scratching (n = 3 per group). BV-2 cells were transfected with nonspecific control (NC) or Fascin-1 (siFascin-1) siRNA for 24 h and treated with or without myelin for an additional 24 h in complete medium. Scale bar: 200 μm. b Quantification of the ratio of the blank area in the scratch migration assay. The results are presented as the mean ± SEM of experiments conducted in triplicate. *P < 0.05 (NC+Myelin or siFascin-1 vs. NC); #P < 0.05 (NC+Myelin vs. siFascin-1). c Transwell assays were

used to detect the migration of microglia. BV-2 cells were treated as described in a. After 48 h, the cells were resuspended in serum-free media and added to the upper chamber. Then, the cells were allowed to migrate for an additional 12 h and stained with crystal violet. Scale bar: 20 μm. d Quantitative analysis of the number of transmembrane cells in c (n = 4 per group). The results are presented as the mean ± SEM. ** P < 0.01 (NC+Myelin vs. NC), * P < 0.05 (siFascin-1 vs. NC). # P < 0.05 (siFascin-1 vs. siFascin-1+Myelin).

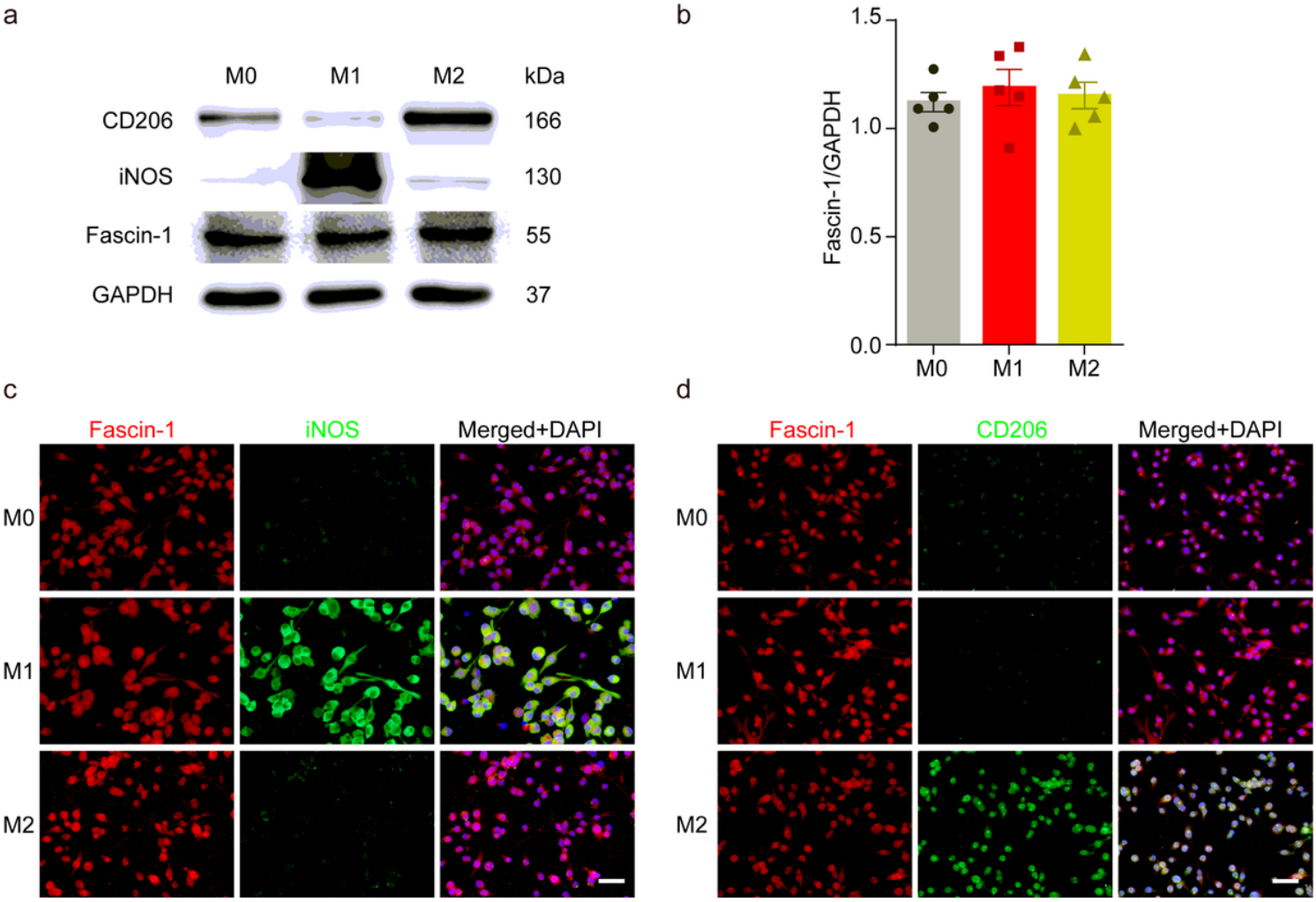

Figure 7

Microglial polarization has no effect on Fascin-1 expression. a Western blot analysis shows the protein expression of M1 (iNOS) or M2 (CD206) polarization markers and Fascin-1 in BV-2 cells after polarization treatment. b Quantitative analysis of Fascin-1 expression in a. GAPDH was used as the loading control. The blots (n = 5 per group) were quantified, as previously described, and no significant difference was observed. c and d Representative immunofluorescence images of M1 (iNOS, Green) or M2 (CD206, Green) markers and Fascin-1 (Red) in BV-2 cells after polarization treatment. The results also indicated no obvious differential expression of Fascin-1. DAPI (Blue) was used to stain the nuclei. Scale bar: 5 μm.